Crystal-field effects and magnetic behavior in $R\mathrm{Ni}_5$ and $R\mathrm{Co}_{5+x}$ rare-earth compounds

P. C. M. Gubbens and A. M. van der Kraan
Delft University of Technology, Interfaculty Reactor Institute, 2629 JB Delft, The Netherlands

K. H. J. Buschow
Philips Research Laboratories, 5600 JA Eindhoven, The Netherlands

(Received 14 June 1988)

Several $R\mathrm{Ni}_5$ and $R\mathrm{Co}_{5+x}$ compounds were studied by rare-earth Mössbauer spectroscopy (^{161}Dy, ^{166}Er, ^{169}Tm). We solved the discrepancy existing in the literature concerning the magnetic ground state in ErNi_5. Two different crystal-field-split level schemes were proposed. Our data showed that the scheme with the $|\pm\frac{15}{2}\rangle$ as ground-state doublet is the correct one. We also found that ErNi_5 and TmNi_5 show slow paramagnetic relaxation above T_c in contrast with DyNi_5, which shows normal relaxation behavior. This difference in relaxation behavior is attributed to differences in the magnetic ground state, being the $|\pm\frac{1}{2}\rangle$ doublet in DyNi_5, while it is the $|\pm\frac{15}{2}\rangle$ doublet in ErNi_5 and the $|\pm 6\rangle$ doublet in TmNi_5. From the lattice contribution of the electric quadrupole splitting in $R\mathrm{Co}_{5+x}$, we determined the concentration dependence of the second-order crystal-field potential A_2^0. Initially it is nearly concentration independent, but decreases for higher x values. For the analysis of the data obtained on $\mathrm{DyCo}_{5.2}$, two second-order terms (A_2^0 and A_2^2) were taken into consideration.

I. INTRODUCTION

Bleaney[1] has already predicted that in $R\mathrm{Ni}_5$ compounds a positive second-order Stevens factor α_J corresponds with an easy c-axis magnetic anisotropy and a negative α_J with an easy-basal-plane magnetic anisotropy. Since then a lot of publications[2–10] have appeared dealing with the crystal-field effects in these compounds. The crystal-field parameters were determined with a variety of experimental techniques, such as inelastic neutron scattering, measurements of the saturation moment, the specific heat, the electrical resistivity, and the magnetic susceptibility. A survey was given by Goremychkin *et al.*[9] In the literature a clear contradiction exists with respect to ErNi_5. On the one hand Escudier *et al.*[4] show that ErNi_5 has an almost pure $|\pm\frac{13}{2}\rangle$ ground state, while on the other hand Goremychkin *et al.*[7] propose $|\pm\frac{15}{2}\rangle$ as the ground state. In order to solve this discrepancy we have measured the temperature dependence of the ^{166}Er Mössbauer spectra of ErNi_5.

The ^{169}Tm Mössbauer spectra of TmNi_5 (which has a very strong uniaxial anisotropy) are characterized by paramagnetic relaxation over a very large temperature range[11] above $T_c=4.5$ K, the latter value being derived from specific-heat data.[8] Therefore, it is of interest to use ^{166}Er and ^{161}Dy Mössbauer spectroscopy in order to study the relaxation behavior in ErNi_5, which has an easy c-axis magnetic anisotropy, and in DyNi_5, which has an easy-basal-plane anisotropy.

From the ^{169}Tm Mössbauer measurements of TmNi_5 we were able to determine the lattice contribution of the electric quadrupole splitting.[11] This value was used subsequently to determine the quantity $(1-\gamma_\infty)/(1-\sigma)=243$, γ_∞ being the Sternheimer antishielding and σ the screening factor. The knowledge of this value makes it possible to derive the second-order crystal-field term B_2^0 from the lattice contribution of the electric quadrupole splitting in various Tm intermetallics, as has been shown, for instance, for Tm_2M_{17} (M=Fe,Co,Ni).[12] Therefore it is of interest to also attempt to determine the values of $(1-\gamma_\infty)/(1-\sigma)$ for ErNi_5 and DyNi_5.

As the atomic number in the rare-earth series increases, a small fraction of the rare-earth atoms in $R\mathrm{Co}_5$ is replaced by Co dumbbell pairs.[13] The influence of this change in composition on the crystal-field potential will be studied by determining this parameter from the lattice contribution of the electric quadrupole splitting in compounds of different Co concentrations.

II. THEORETICAL ASPECTS

The crystal field of trivalent Dy and Er ($J=\frac{15}{2}$) for hexagonal symmetry can be described by means of the Hamiltonian

$$H_c=B_2^0O_2^0+B_4^0O_4^0+B_6^0O_6^0+B_6^6O_6^6\ , \tag{1}$$

where O_n^m are operator equivalents[14] and $B_n^m=\theta_n V_n^m=\theta_n\langle r^n\rangle A_n^m$, and where θ_n represents the Stevens constants α_J, β_J, and γ_J for $n=2$, 4, and 6, respectively.[14] The symbol $\langle r^n\rangle$ represents Hartree-Fock radial integrals[15] and A_n^m are the crystal-field potentials.

When we include the interaction of rare-earth moments with the molecular field present at these sites, the Hamiltonian H becomes

$$H=H_c-g_J\mu_B\mathbf{H}_M\cdot\mathbf{J}\ . \tag{2}$$

In this expression the quantity g_J is the Landé g factor and H_M is the molecular field. The energy levels with

corresponding eigenfunctions can be determined after diagonalization of the Hamiltonian. Furthermore, the energy levels and their eigenfunctions determine the temperature dependencies of the hyperfine field and the quadrupole splitting via the expressions

$$H_{\rm eff}(T)=H_{\rm eff}(0)|\langle J_z\rangle_{\rm av}|/J \tag{3}$$

and

$$\Delta_{\rm QS}(T)=\Delta_{\rm QS}^{4f}(0)\frac{\langle 3J_z^2-J(J+1)\rangle_{\rm av}}{J(2J-1)}+\Delta_{\rm QS}^{\rm latt}\ , \tag{4}$$

where $\langle\ \rangle_{\rm av}$ indicates a thermal average over the energy levels of the crystal-field scheme. From the lattice contribution of the quadrupole splitting $\Delta_{\rm QS}^{\rm latt}=\frac{1}{2}eV_{zz}^{\rm latt}Q$ by using $Q=+2.35\times10^{-24}$ cm^2 for ^{161}Dy, $Q=-1.59\times10^{-24}$ cm^2 for ^{166}Er, and $Q=-1.20\times10^{-24}$ cm^2 for ^{169}Tm (Ref. 16) one may determine the lattice contribution of the principal component of the electric-field-gradient tensor $V_{zz}^{\rm latt}$. The relation with the crystal-field parameter is given by

$$eV_{zz}^{\rm latt}=-\frac{1-\gamma_\infty}{1-\sigma}\frac{2V_2^0}{\langle r^2\rangle}[3\cos^2\theta-1+\eta\sin^2\theta\cos(2\varphi)]\ , \tag{5}$$

where the angles θ,φ define the easy magnetization direction relative to the axis of the electric-field-gradient tensor and where η is the asymmetry parameter. The following values were used for the Hartree-Fock radial integrals:[15] $\langle r^2\rangle=0.726$ a.u.^{2} for Dy, $\langle r^2\rangle=0.666$ a.u.^{2} for Er, and $\langle r^2\rangle=0.646$ a.u.^{2} for Tm. In this formula $\eta=V_2^2/V_2^0$. For hexagonal crystal structure (RNi$_5$) the symmetry is axial and hence $\eta=0$. In the case of an easy magnetization axis parallel to the c axis, one has $\theta=0$ and formula (5) can be written as

$$eV_{zz}^{\rm latt}=-\frac{1-\gamma_\infty}{1-\sigma}\frac{4V_2^0}{\langle r^2\rangle}=-\frac{1-\gamma_\infty}{1-\sigma}4A_2^0\ . \tag{6}$$

III. EXPERIMENT

The RNi$_5$ and RCo$_{5+x}$ samples were prepared by arc melting the 99.9%-pure starting materials in an atmosphere of purified argon gas. After annealing, the samples were examined by x-ray diffraction and found to be single phase.

The ^{161}Dy, ^{166}Er, and ^{169}Tm Mössbauer spectra were obtained by means of acceleration-type spectrometers in sinusoidal mode, though the measured points were plotted on a linear scale.

The velocity of the ^{161}Dy and ^{169}Tm spectrometers was calibrated in an absolute sense with a laser Michelson interferometer. The ^{161}Dy Mössbauer effect was measured using 25.6-keV gamma rays emitted by ^{161}Tb obtained after neutron irradiation of ^{160}Gd$_{0.5}$^{163}Dy$_{0.5}$Fe$_3$. The 25.6-keV gamma rays were detected by means of a Ge detector. The ^{169}Tm Mössbauer effect was measured using 8.4-keV gamma rays emitted by ^{169}Er obtained after neutron irradiation of a ^{168}ErAl$_3$-6Al foil. The 8.4-keV gamma rays were detected by means of a Si(Li) detector, which discriminates the 8.4-keV gamma rays very well with respect to the erbium L lines. The ^{166}Er Mössbauer effect was measured using the 80.6-keV gamma rays emitted by ^{166}Ho obtained after neutron irradiation of a small sample of cubic HoPd$_3$. The 80.6-keV gamma rays were detected by means of a Ge detector. The ^{166}Er Mössbauer spectra were measured in a cryostat, in which both source and absorber were mounted at liquid-helium temperature. The temperature dependence of the absorber was regulated independently with respect to the source, which was kept at $T=4.2$ K. The velocity was calibrated by measuring the ^{166}Er Mössbauer spectra of ErFe$_2$, which has a hyperfine field of 840 T,[17] which corresponds to an overall splitting of 12.44 cm/s.

IV. EXPERIMENTAL RESULTS

Figure 1 shows some representative examples of the ^{166}Er Mössbauer spectra of ErNi$_5$ measured between $T=4.2$ and 75 K. The spectra measured below and above T_c show a clear five-line pattern. The Curie temperature reported for ErNi$_5$ equals $T_c=8$ K as derived from specific-heat data[2] and $T_c=10$ K as derived from magnetization measurements.[6] With increasing temperature the spectra show an increasing broadening. This behavior is typical for paramagnetic relaxation. No hysteresis has been found in ErNi$_5$. The spectra were analyzed with a modified spin-up and spin-down relaxation model of Blume and Tjon.[18]

Figure 2 shows several representative ^{161}Dy Mössbauer spectra of DyNi$_5$ measured between $T=2.4$ and 20 K. At $T=2.4$ K the spectrum of DyNi$_5$ has sharp lines; these lines show an increasing broadening with increasing

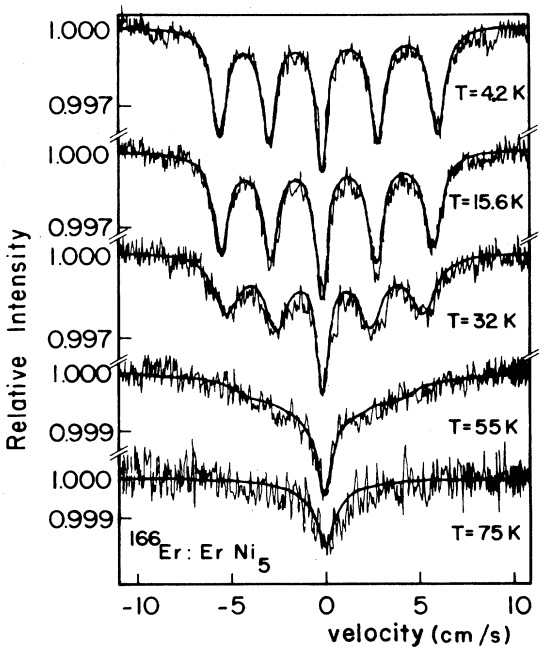

FIG. 1. ^{166}Er Mössbauer spectra of ErNi$_5$. The solid curve is a fit obtained with a spin-up–spin-down relaxation model.

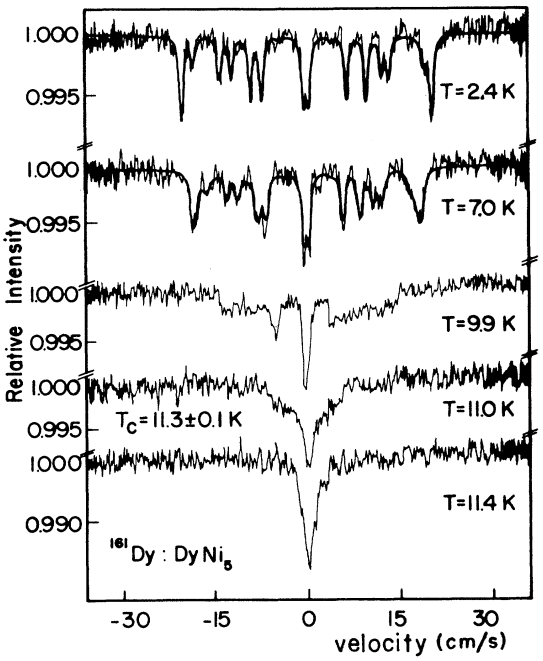

FIG. 2. ^{161}Dy Mössbauer spectra of $DyNi_5$.

temperature due to electronic relaxation. The Curie temperature of $DyNi_5$ is $T_c = 11.3 \pm 0.1$ K. Above this temperature a single broadened line is expected and was observed.

In Fig. 3 the temperature dependence of the hyperfine and the quadrupole splitting of ^{166}Er Mössbauer spectra are shown, while Fig. 4 shows the temperature dependence of the hyperfine splitting of the ^{161}Dy, ^{166}Er, and ^{169}Tm Mössbauer spectra of $DyNi_5$, $ErNi_5$, and $TmNi_5$, respectively.

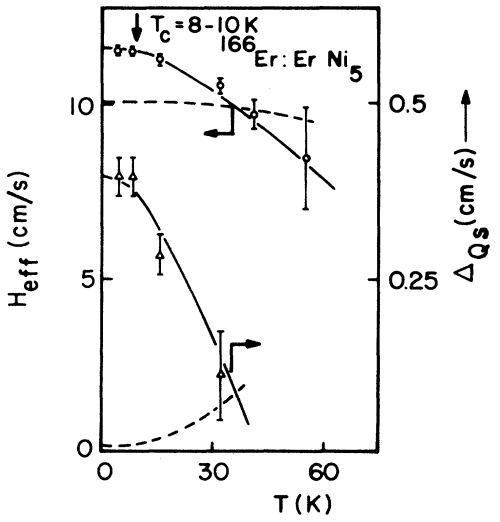

FIG. 3. The temperature dependence of the measured hyperfine field and electric quadrupole splitting of $ErNi_5$. The solid and dashed curves are explained in the text.

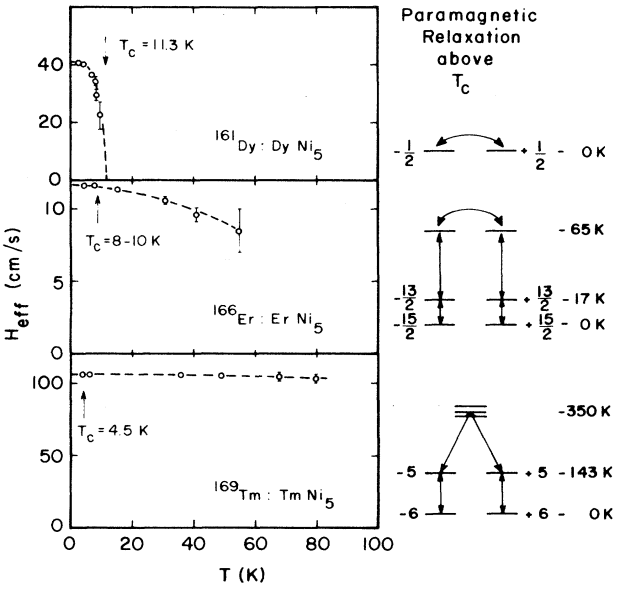

FIG. 4. The temperature dependence of the hyperfine field in three RNi_5 compounds. The dashed lines are drawn to guide the eye. On the right the corresponding crystal-field diagrams are given. The double arrows indicate nonzero transition probabilities.

In Fig. 5 the ^{166}Er and ^{169}Tm Mössbauer spectra obtained at 4.2 K for $ErCo_{5.9}$ and $TmCo_{6.1}$ are shown. The spectrum of $ErCo_{5.9}$ is slightly broadened at the outside regions while no clear line broadening is found in $TmCo_{6.1}$.

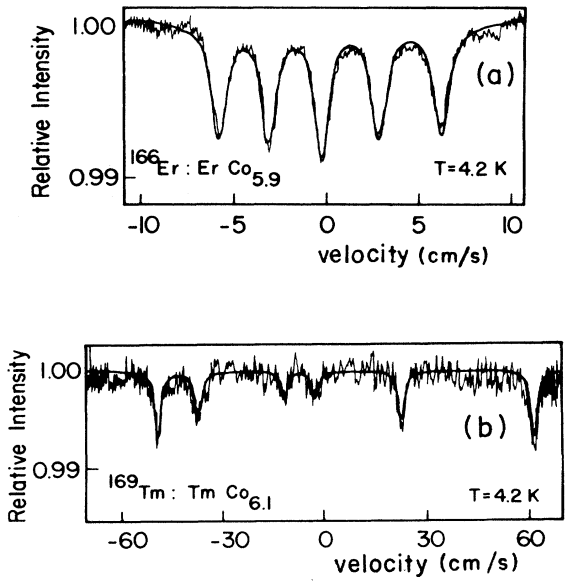

FIG. 5. (a) ^{166}Er Mössbauer spectrum of $ErCo_{5.9}$ at $T = 4.2$ K. (b) ^{169}Tm Mössbauer spectrum of $TmCo_{6.1}$ at $T = 4.2$ K.

TABLE I. Hyperfine field (H_{eff}) and electric quadrupole splitting ($\frac{1}{2}e^2qQ$) derived from fits of the ^{161}Dy spectra of $DyNi_5$ and $DyCo_{5.2}$, the ^{166}Er spectra of $ErNi_5$ and $ErCo_{5.9}$, and the ^{169}Tm spectrum of $TmCo_{6.1}$. All values refer to 4.2 K, except those of $DyNi_5$ (2.4 K).

Compound	H_{eff} (cm/s)	H_{eff} (T)	$\frac{1}{2}e^2qQ$ (cm/s)
$DyNi_5$	40.1±0.5	507±6	4.0±0.2
$DyCo_{5.2}$	47.6±0.5	600±6	6.1±0.2
Free ion	44.5	565	7.0
$ErNi_5$	11.6±0.1	785±7	0.40±0.05
$ErCo_{5.9}$	11.9±0.1	805±7	0.55±0.05
Free ion	11.60	785	0.81
$TmCo_{6.1}$	119.7±0.5	743±4	14.6±0.3
Free ion	116.0	720	15.7

In Table I we have listed the values of the hyperfine fields and the electric quadrupole splittings of the RNi_5 and RCo_{5+x} compounds together with the corresponding free-ion values. The values of $DyNi_5$ refer to measurements obtained at $T=2.4$ K, while the other values refer to $T=4.2$ K. The values of $DyCo_{5.2}$ are about the same as those obtained earlier by Novik and Wernick,[19] while the values of $DyNi_5$ are smaller than those reported by these authors.

The free-ion values of the Er hyperfine field and the Er quadrupole splitting are 785 T (11.6 cm/s) and 0.81 cm/s, respectively.[20] An additional check of these values was made by comparing the values obtained from the ^{166}Er spectrum of Er_2Fe_{17} with those of the ^{169}Tm spectrum of Tm_2Fe_{17}.[12] The free-ion values of ^{161}Dy and ^{169}Tm were taken from Refs. 12 and 21. The free-ion values in Table I were estimated on the basis of $|J_z=-\frac{15}{2}\rangle$ for Er and Dy and $|J_z=-6\rangle$ for Tm under the assumption $B_n^m=0$ and are proportional to $M=gJ_z$.

V. DISCUSSION

A. RNi_5 compounds

As already mentioned briefly in the Introduction there is a discrepancy between Refs. 4 and 7 regarding the character of the ground-state doublet in $ErNi_5$ and the corresponding crystal-field diagram. Escudier *et al.*[4] measured the saturation magnetization and the temperature dependence of the magnetic susceptibility on a single crystal and also performed inelastic neutron scattering. From these results and also from slightly modified data of Gignoux *et al.*[6] it can be concluded that the ground-state doublet in $ErNi_5$ is $|\pm\frac{13}{2}\rangle$. At an energy of 30 K, two excited levels occur consisting of almost pure $|\pm\frac{15}{2}\rangle$ and $|\pm\frac{11}{2}\rangle$ states. On the other hand, Goremychkin *et al.*[7] found on the basis of inelastic neutron scattering an almost pure $|\pm\frac{15}{2}\rangle$ ground-state doublet. The first excited state is the $|\pm\frac{13}{2}\rangle$ level, located at an energy of 17 K above the ground state, the remainder of levels being found at excitation energies higher than 65 K. Such a ground-state doublet would be in disagreement with the conclusions derived from the magnetization measurements of Escudier *et al.*[4]

In Table II we have tabulated the crystal-field parameters obtained by Escudier *et al.* and Goremychkin *et al.* A detailed calculation of the relative influence of the various terms shows that in the case of Escudier *et al.*[4] the B_6^0 term causes the $|\pm\frac{13}{2}\rangle$ to be lower than the $|\pm\frac{15}{2}\rangle$ doublet. The latter ground state would be excited if only B_2^0 is important. The main difference between the two sets of values is that B_4^0 in the case of Goremychkin *et al.*[7] is much larger than in Ref. 4. One may note that in this case B_4^0 effectively compensates the influence of B_6^0 in order to achieve again a $|\pm\frac{15}{2}\rangle$ doublet ground state.

We have compared the experimental temperature dependences of the hyperfine field and quadrupole splitting of $ErNi_5$ with those calculated on the basis of formulas (1), (3), and (4) and the crystal-field parameters tabulated in Table II. In Fig. 3 we show the curves calculated on the basis of the parameters of Goremychkin *et al.* (solid lines) and those of Escudier *et al.* (dashed lines). It may be seen that a good fit is obtained with the level scheme proposed by Goremychkin *et al.*, while no satisfactory result is obtained when using the scheme of Escudier *et al.*

From Table I it appears that the lattice contribution of the electric quadrupole splitting for $ErNi_5$ (the difference between free-ion value and the measured value) is -0.41 ± 0.05 cm/s. From the data published by Goremychkin *et al.*[7] one derives a value of B_2^0 equal to -0.64 ± 0.05 K. Inserting these values into formula (6) one finds $(1-\gamma_\infty)/(1-\sigma)=270\pm30$. This value is in good agreement with the value $(1-\gamma_\infty)/(1-\sigma)=243$ found by us in $TmNi_5$.[11]

From Table I it appears that the hyperfine field and quadrupole splitting of the ^{161}Dy Mössbauer spectrum in $DyNi_5$, measured at $T=2.4$ K, are reduced with respect to the free-ion values. This behavior can be explained in the same manner as described earlier by Bogé *et al.*[22] for Dy_2Ni_{17}, which, just like $DyNi_5$, has an easy magnetization direction perpendicular to the c axis. Since no experimental data exist of the crystal field and diagram of $DyNi_5$, we have extrapolated the values of $TbNi_5$ (Refs. 6, 7, and 9) and $HoNi_5$ (Ref. 5) to $DyNi_5$, which leads to a $|\pm\frac{1}{2}\rangle$ ground-state doublet. Since the data for $ErNi_5$ showed that transferred hyperfine fields are negligible, we deduce from the experimental hyperfine field of $DyNi_5$ an effective $\langle J_x\rangle$ value equal to 6.7. Using the crystal parameters of $DyNi_5$ after extrapolation from the $TbNi_5$ data, we calculate by an iterative procedure with formula (2) a value equal to $\langle J_x\rangle=6.7$ and a corresponding value of $g_J\mu_B H_M=7$ K. Using $T_c=11.3\pm0.3$ K it is possible to calculate $g_J\mu_B H_M$ with a molecular field approximation by means of the relation

$$g_J\mu_B H_M=3kT_c\frac{\langle J_x\rangle}{J(J+1)}\ . \tag{7}$$

These calculations give $g_J\mu_B H_M=3.5$ K, which is half the value found above. Calculation of the quadrupole splitting gives a value of 4.9 cm/s. Since the experimen-

TABLE II. Comparison of the crystal-field parameters of $ErNi_5$ (a) as proposed by P. Escudier *et al.* [Physica B+C **86-88B**, 197 (1977)] and (b) as proposed by F. A. Goremychin *et al.* [Phys. Status Solidi B **121**, 623 (1984)].

Parameter	(a)	(b)
B_2^0 (K)	-0.7 ± 0.1	-0.64 ± 0.05
B_4^0 (K)	$(-1\pm2)\times10^{-3}$	$(-2.27\pm0.20)\times10^{-3}$
B_6^0 (K)	$(0.5\pm0.2)\times10^{-4}$	$(0.23\pm0.02)\times10^{-4}$
B_6^6 (K)	$(3\pm1)\times10^{-4}$	$(1.3\pm0.2)\times10^{-4}$

tal value is 4.0±0.2 cm/s, this gives a lattice contribution of −0.9±0.2 cm/s. In $DyNi_5$ the easy axis of magnetization is perpendicular to the c axis so that formula (5) can be written as $eV_{zz}=-[(1-\gamma_\infty)/(1-\sigma)]2V_2^0/\langle r^2\rangle$. If we use $B_2^0=2.3$ K for $DyNi_5$ as extrapolated from the $TbNi_5$ data[6] we find $(1-\gamma_\infty)/(1-\sigma)=230\pm80$ K. Approximately this value is still in the range of values determined earlier for $ErNi_5$ and $TmNi_5$.[11] However, when we would have used the B_2^0 value extrapolated from that of $HoNi_5$ (Ref. 5) we would have found a value which is 30% smaller, showing the limitations of this procedure.

It can be seen from Fig. 4 that $DyNi_5$ orders magnetically below $T_c=11.3$ K and shows a hyperfine field splitting and hence no paramagnetic relaxation above this temperature. By contrast, the data shown for $ErNi_5$ and $TmNi_5$ in Fig. 4 reveal hyperfine splitting to be present in an extended temperature range above T_c. Also, the hyperfine-split spectra become broadened with increasing temperature. All these phenomena are attributed to slow paramagnetic relaxation. It is well known and it has been shown in detail by Birgeneau[23] that transition probabilities are proportional to $|\langle\phi_i|J|\phi_j\rangle|^2$ and take nonzero values only between crystal-field levels if J represents J_+, J_-, or J_z. As shown in Fig. 4 this means that in the case of $DyNi_5$ a direct transition path exists between the two levels of the ground-state doublet, while in the cases of $ErNi_5$ and $TmNi_5$ only an indirect path is possible. In $ErNi_5$ there is a transition probability between the states $|+\frac{15}{2}\rangle$ and $|-\frac{15}{2}\rangle$ via the excited state at an energy of 65 K, which is a doublet with the eigenfunctions $0.141|\pm\frac{13}{2}\rangle+0.826|\pm\frac{1}{2}\rangle-0.552|\mp\frac{11}{2}\rangle$. In $TmNi_5$,[8] however, a similar transition path can take place only for excitation energies of about 350 K. One may expect, therefore, that this kind of indirect trajectory gives a longer relaxation time in $TmNi_5$ than in $ErNi_5$. This agrees with experimental observations. In $TmNi_5$ one observes relaxation effects up to about 250 K and in the case of $ErNi_5$ only up to about 60 K. For an accurate determination of the corresponding relaxation times a fairly complex electronic relaxation model is required, our interpretation in terms of spin-up and spin-down levels being only a first approximation.

B. RCo_{5+x} compounds

In Table III we have tabulated the V_{zz}^{latt} terms as derived from the experimental data by means of the formula $\Delta_{QS}=\frac{1}{2}e^2V_{zz}Q$. The values of $GdCo_5$ and Gd_2Co_{17} were taken from the data published by Tomala *et al.*,[24] while the value of Tm_2Co_{17} was taken from Ref. 12. The values listed for the factor $(1-\gamma_\infty)/(1-\sigma)$ for Er and Tm were derived from ^{166}Er and ^{169}Tm Mössbauer measurements of $ErNi_5$ and $TmNi_5$, as explained above. These factors are about 60% larger than those derived theoretically by Gupta and Sen.[25] In a similar way we are able to give now an experimental estimate also of the $(1-\gamma_\infty)/(1-\sigma)$ factors for Gd and Dy, as shown in Table III. With formula (5) we calculated subsequently the crystal-field potential A_2^0. These A_2^0 values have been plotted as a function of Co concentration in Fig. 6. These results are in good agreement with the value $A_2^0=-230\pm50$ K found for $SmCo_5$.[26] In the case of $DyCo_{5.2}$ (that has an easy a-axis magnetization[27]) we have used the value calculated for A_2^0 and neglected the asymmetric term A_2^2, although such a term very likely is present for this moment direction in $DyCo_{5.2}$. As explained earlier, the A_2^2 term plays no role in the case of $ErCo_{5.9}$ and $TmCo_{6.1}$, since in these compounds the easy magnetization direction is parallel to the c axis. From Fig. 5 it appears that the A_2^0 value of $DyCo_{5.2}$ is larger than expected on the basis of the other data given in this figure. If we were to interpolate for $DyCo_{5.2}$ a value of $A_2^0=-210$ K we would find $A_2^2=190\pm100$ K.

From the data of Fig. 5 it appears that the A_2^0 term is initially approximately constant until $x\approx1$ in RCo_{5+x}, but then starts to decrease with increasing x. From this behavior we conclude that small amounts of Co dumbbell pairs in RCo_5 compounds have hardly any influence on the magnetic rare-earth sublattice anisotropy.

VI. CONCLUDING REMARKS

The analysis given for $ErNi_5$ makes it clear that a combination of techniques providing local sampling and bulk

TABLE III. Lattice contributions of V_{zz}, $(1-\gamma_\infty)/(1-\sigma)$ values, and corresponding calculated crystal-field potentials A_2^0 for RCo_{5+x} compounds. The data for Tm_2Co_{17} were taken from the results published earlier by P. C. M. Gubbens *et al.* [J. Magn. Magn. Mater. **67**, 255 (1987)].

Compound	V_{zz}^{latt} (10^{17} cm^{-2})	$\frac{1-\gamma_\infty}{1-\sigma}$	A_2^0 (K)
$GdCo_5$	+8.2	320	−206
$DyCo_{5.2}$	−7±2	285	−400±100
$ErCo_{5.9}$	+8.0±1.5	270	−230±50
$TmCo_{6.1}$	+5.6±1.0	243	−185±30
$TmCo_{8.5}$ (Tm_2Co_{17})	+4.2±1.0 +1.4±1.0	243	−140±30 −47±30
$GdCo_{8.5}$ (Gd_2Co_{17})	+4.3	320	−108

sampling is sometimes required for deriving the correct crystal-field-split level schemes. We showed that the results obtained for $ErNi_5$ by Mössbauer spectroscopy are important supplementary data for the correct interpretation of neutron scattering data. A second interest in compounds such as $ErNi_5$ and $TmNi_5$ arises from our observation that these materials exhibit paramagnetic relaxation phenomena over quite extended temperature ranges and for this reason might serve as a test ground for "indirect" relaxation models. Based on the prediction of Bleaney,[1] similar paramagnetic relaxation phenomena can be expected, for instance also for $SmNi_5$, owing to its easy c-axis magnetization, but not for $NdNi_5$, where the easy magnetization direction is perpendicular to the c axis.

Finally, we note that the lattice contribution to the quadrupole splitting, in particular, is a very useful tool for determining the lower-order crystal-field terms.

The data in Fig. 6 give a good impression as to the sensitivity of the different types of rare-earth Mössbauer isotopes. It is clear that ^{155}Gd is the most sensitive one, since no orbital and hence no $4f$ contribution is present. In the other cases the lattice contribution had to be separated from the $4f$ contribution and it appears that the sensitivity decreases in the sequence ^{169}Tm, ^{166}Er, and ^{161}Dy. In order to have the availability of more accurate empirical values of the factor $(1-\gamma_\infty)/(1-\sigma)$ additional experiments will be needed, preferentially made on hexagonal compounds using a combination of rare-earth Mössbauer spectroscopy and inelastic neutron scattering.

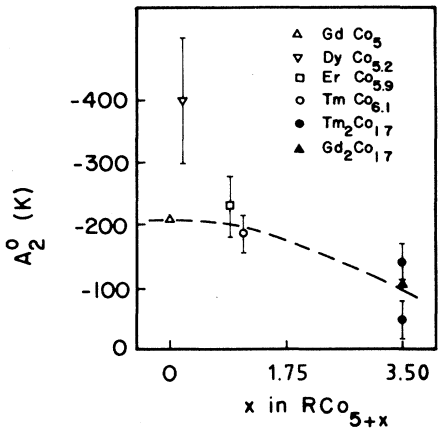

FIG. 6. The values determined for A_2^0 as function of x in RCo_{5+x}. The dashed curve is drawn to guide the eye.

ACKNOWLEDGMENTS

The authors are indebted to Edo Gerkema for his assistance with the ^{166}Er Mössbauer-effect measurements.

[1] B. Bleaney, Proc. Phys. Soc., London **82**, 469 (1969).
[2] S. G. Sankar, D. A. Keller, R. S. Craig, W. E. Wallace, and V. U. S. Rao, J. Solid State Chem. **9**, 78 (1974).
[3] P. A. Alekseev, A. Andreeff, H. Griesmann, L. P. Kaun, B. Lippold, W. Matz, I. P. Sadikov, O. D. Chistyakov, I. A. Marova, and E. M. Savitskii, Phys. Status Solidi B **97**, 87 (1980).
[4] P. Escudier, D. Gignoux, D. Givord, R. Lemaire, and A. P. Murani, Physica B+C **86-88B**, 197 (1977).
[5] E. A. Goremychkin, E. Mühle, B. Lippold, O. D. Chistyakov, and E. M. Savitskii, Phys. Status Solidi B **127**, 371 (1985).
[6] D. Gignoux, A. Nait-Saada, and R. Perrier de la Bâthie, J. Phys. (Paris) Colloq. **40**, C5-188 (1979).
[7] F. A. Goremychkin, E. Mühle, P. G. Ivanitskii, V. T. Krotenko, M. V. Pasechnik, V. V. Slisenko, A. A. Vasilkevich, B. Lippold, O. D. Chistyakov, and E. M. Savitskii, Phys. Status Solidi B **121**, 623 (1984).
[8] D. Gignoux, B. Hennion, and A. Nait-Saada, in *Proceedings of the Conference on Crystal Electric Field Effects, Wrocław, Poland* (Plenum, New York, 1982), p. 485.
[9] E. A. Goremychkin *et al.*, Report of the Joint Institute of Nuclear Research, Dubna, 1984, No. P 14-84-632 (unpublished).
[10] D. Gignoux and J. J. Rhyne (private communication).
[11] P. C. M. Gubbens, A. M. van der Kraan, and K. H. J. Buschow, J. Magn. Magn. Mater. **50**, 199 (1985).
[12] P. C. M. Gubbens, A. M. van der Kraan, J. J. van Loef, and K. H. J. Buschow, J. Magn. Magn. Mater. **67**, 255 (1987).
[13] K. H. J. Buschow and W. A. J. J. Velge, Z. Angew. Phys. **26**, 157 (1969).
[14] K. W. H. Stevens, Proc. Phys. Soc., London, Sect. A **65**, 109 (1952).
[15] A. J. Freeman and R. E. Watson, Phys. Rev. **127**, 2058 (1962).
[16] *Mössbauer Effect Data Index*, edited by J. G. Stevens and V. E. Stevens (Plenum, New York, 1974).
[17] P. J. Viccaro, G. K. Shenoy, B. D. Dunlap, D. G. Westlake, and J. F. Miller, J. Phys. (Paris) Colloq. **40**, C2-198 (1979).
[18] M. Blume and J. A. Tjon, Phys. Rev. **165**, 446 (1968).
[19] I. Novik and J. H. Wernick, Phys. Rev. **140**, A131 (1965).
[20] G. Petrich, Z. Phys. **221**, 431 (1969).
[21] P. C. M. Gubbens, A. M. van der Kraan, and K. H. J. Buschow, Phys. Status Solidi B **130**, 575 (1985).
[22] M. Bogé, J. Chappert, A. Yaouanc, and J. M. D. Coey, Solid State Commun. **31**, 987 (1979).
[23] R. J. Birgenau, J. Phys. Chem. Solids **33**, 59 (1972).
[24] K. Tomala, G. Czjzek, J. Fink, and H. Schmidt, Solid State Commun. **24**, 857 (1977).
[25] R. P. Gupta and S. K. Sen, Phys. Rev. A **7**, 850 (1973).
[26] J. X. Boucherle, D. Givord, J. Laforest, J. Schweizer, and F. Tasset, J. Phys. (Paris) Colloq. **40**, C5-180 (1979).
[27] M. Ohkoski, H. Kobayashi, T. Katayama, M. Hirano, and T. Tsushima, Physica B+C **86-88B**, 195 (1977).